

See discussions, stats, and author profiles for this publication at: <https://www.researchgate.net/publication/8064871>

Wetting and Self-Cleaning Properties of Artificial Superhydrophobic Surfaces

ARTICLE *in* LANGMUIR · MARCH 2005

Impact Factor: 4.46 · DOI: 10.1021/la0401011 · Source: PubMed

CITATIONS

652

READS

295

4 AUTHORS, INCLUDING:



Wilhelm Barthlott

University of Bonn

525 PUBLICATIONS **13,024** CITATIONS

SEE PROFILE



Peter Walzel

Technische Universität Dortmund

170 PUBLICATIONS **1,216** CITATIONS

SEE PROFILE

Wetting and Self-Cleaning Properties of Artificial Superhydrophobic Surfaces

Reiner Fürstner* and Wilhelm Barthlott

Nees-Institut für Biodiversität der Pflanzen, Rheinische Friedrich-Wilhelms-Universität Bonn,
Meckenheimer Allee 170, D-53115 Bonn, Germany

Christoph Neinhuis

Institut für Botanik, Technische Universität Dresden, D-01069 Dresden, Germany

Peter Walzel

Lehrstuhl für Mechanische Verfahrenstechnik, Fachbereich Bio- und Chemieingenieurwesen,
Universität Dortmund, Emil-Figge-Str. 68, D-44227 Dortmund, Germany

Received July 20, 2004. In Final Form: October 19, 2004

The wetting and the self-cleaning properties (the latter is often called the “Lotus-Effect”) of three types of superhydrophobic surfaces have been investigated: silicon wafer specimens with different regular arrays of spikes hydrophobized by chemical treatment, replicates of water-repellent leaves of plants, and commercially available metal foils which were additionally hydrophobized by means of a fluorinated agent. Water droplets rolled off easily from those silicon samples which had a microstructure consisting of rather slender spikes with narrow pitches. Such samples could be cleaned almost completely from artificial particulate contaminations by a fog consisting of water droplets (diameter range, 8–20 μm). Some metal foils and some replicates had two levels of roughening. Because of this, a complete removal of all particles was not possible using artificial fog. However, water drops with some amount of kinetic impact energy were able to clean these surfaces perfectly. A substrate where pronounced structures in the range below 5 μm were lacking could not be cleaned by means of fog because this treatment resulted in a continuous water film on the samples.

Introduction

After some time virtually all surfaces in a natural environment get contaminated. Cleaning them requires high efforts; additionally, often surfactants are applied with negative effects on the environment.

Some years ago our group showed that the leaves of several plants are cleaned completely from dust pollutions by a simple rain shower.¹ Such leaves are called “superhydrophobic”; that is, water droplets form spheres with very little adhesion to the surface and roll off very quickly even at small inclinations. A main characteristic of superhydrophobic surfaces is a roughness on the micro- and nanometer scales. Water droplets as well as dirt particles only lie on the tips of these structures. Therefore, contaminating particles develop low adhesion forces to such rough surfaces and can be removed very effectively by rain.

The principal connections between surface roughness and water repellency were worked out by Cassie and Baxter,² as well as Wenzel.³ Until now many authors have contributed to a better understanding of the behavior of water on superhydrophobic surfaces.^{4–12} Methods to create

artificial superhydrophobic surfaces are described in numerous reports.^{13–19} However, only very few investigations on the self-cleaning properties of artificial superhydrophobic surfaces have been published yet. Nakajima et al.²⁰ reported about self-cleaning superhydrophobic surfaces although the term “self-cleaning” means something different here: it is the photocatalytic effect due to the presence of TiO_2 which was a component of the described coating.

In the present study, we determined the wetting and the self-cleaning properties of three types of superhydrophobic surfaces. As a model system with a simple geometry of the microstructure we used silicon wafer specimens with different regular arrays of spikes which were made hydrophobic. Starting from water-repellent leaves of

* To whom correspondence should be addressed. Present address: STO AG, Standort Kriftel, Abt. TIGF, Gutenbergstr. 6, D-65830 Kriftel, Germany. E-mail: r.fuerstner@stoeu.com.

(1) Barthlott, W.; Neinhuis, C. *Planta* **1997**, *202*, 1.
(2) Cassie, A. B. D.; Baxter, S. *Trans. Faraday Soc.* **1944**, *40*, 546.
(3) Wenzel, T. N. *J. Phys. Colloid Chem.* **1949**, *53*, 1455.
(4) Adam, N. K. Principles of Water-repellency. In *Water-Proofing and Water-Repellency*; Moilliet, J. L., Ed.; Elsevier Publishing Company: Amsterdam, 1963; p 1.
(5) Bico, J.; Marzolin, C.; Quéré, D. *Europhys. Lett.* **1999**, *47*, 220.
(6) Chen, W.; Fadeev, A. Y.; Hsieh, M. C.; Oner, D.; Youngblood, J.; McCarthy, T. J. *Langmuir* **1999**, *15*, 3395.

(7) Herminghaus, S. *Europhys. Lett.* **2000**, *52*, 165.
(8) Lafuma, A.; Quéré, D. *Nat. Mater.* **2003**, *2*, 457.
(9) Oner, D.; McCarthy, T. J. *Langmuir* **2000**, *16*, 7777.
(10) Patankar, N. A. *Langmuir* **2003**, *19*, 1249.
(11) Patankar, N. A. *Langmuir* **2004**, *20*, 8209.
(12) Richard, D.; Quéré, D. *Europhys. Lett.* **1999**, *48*, 286.
(13) Nakajima, A.; Fujishima, A.; Hashimoto, K.; Watanabe, T. *Adv. Mater.* **1999**, *11*, 1365.
(14) Ogawa, K.; Soga, M.; Takada, Y.; Nakayama, I. *Jpn. J. Appl. Phys.* **1993**, *32*, L614.
(15) Onda, T.; Shibuichi, S.; Satoh, N.; Tsujii, K. *Langmuir* **1996**, *12*, 2125.
(16) Shibuichi, S.; Yamamoto, T.; Onda, T.; Tsujii, K. *J. Colloid Interface Sci.* **1998**, *208*, 287.
(17) Tadanaga, K.; Katata, N.; Minami, T. *J. Am. Ceram. Soc.* **1997**, *80*, 1040.
(18) Yamauchi, G.; Miller, J. D.; Saito, H.; Takai, K.; Ueda, T.; Takazawa, H.; Yamamoto, H.; Nishii, S. *Colloids Surf., A* **1996**, *116*, 125.
(19) Youngblood, J. P.; McCarthy, T. J. *Macromolecules* **1999**, *32*, 6800.
(20) Nakajima, A.; Hashimoto, K.; Watanabe, T.; Takai, K.; Yamauchi, G.; Fujishima, A. *Langmuir* **2000**, *16*, 7044.

Table 1. Designations and Prescribed and Actual Dimensions of the Silicon Chips with Regular Patterns of Spikes^a

designation	prescribed dimensions		actual dimensions					
			$h = 1 \mu\text{m}$		$h = 2 \mu\text{m}$		$h = 4 \mu\text{m}$	
	d [μm]	a [μm]	d [μm]	a [μm]	d [μm]	a [μm]	d [μm]	a [μm]
d_1a_1	1	1	0.85	1.05	0.89	1.01	0.90	1.01
$d_1a_{1.5}$	1	1.5	0.77	1.59	0.85	1.55	0.84	1.53
d_1a_2	1	2	0.9	1.97	0.92	1.93	0.94	1.85
d_1a_3	1	3	0.88	2.89	0.92	2.89	0.96	2.90
d_1a_5	1	5	0.75	4.91	0.88	4.86	0.92	4.82
d_2a_2	2	2	1.94	1.88	1.94	1.89	2.02	1.91

^a d , width; a , clearance; h , height (referring to the top side of the spikes).

plants we prepared replicates; these are more durable than the originals on one hand, and on the other hand, all replicates, made of a hydrophobic polymer, have the same surface chemistry, allowing the comparison of the effect of different microstructure geometries on water repellency and self-cleaning. The third type of surfaces was commercially available metal foils normally used for printed electronic circuits or condensers additionally hydrophobized by means of a fluorinated agent.

Experimental Section

Preparation of the Surfaces. Silicon wafer specimens with regular patterns of spikes were manufactured by X-ray lithography (Fraunhofer Institute Silicon Technology—ISIT, Itzehoe, Germany). The distance a between the spikes as well as their width d and their height h were varied. Table 1 shows the prescribed and the actual dimensions of 18 different types of structuring, the latter measured by means of a scanning electron microscope (SEM); the width of the spikes was measured near their top side. The $1\text{-}\mu\text{m}$ diameter spikes had an almost cylindrical shape as in Figure 1a; spikes of $2\text{-}\mu\text{m}$ width represented prisms with a nearly square base, as in Figure 1b. The silicon specimens had a size of 13×18 mm. They were hydrophobized with Au-thiol (for a description, see Table 2).

Replicates of plant surfaces were made by means of a two-component silicon molding mass (President light body, Coltene, Switzerland) applied onto the leaf's surface. After curing, the negative is flexible and rubberlike. Onto this mold a melted polymer (polyether, ZK 2068-026, BASF, Germany) was applied. Because the polymer was highly hydrophobic no subsequent hydrophobizing treatment of the replicate was necessary (for designations, see Table 3).

Two metal specimens examined in our experiments were manufactured for printed electronic circuits representing copper foils with a smooth upper surface and a heavily structured lower surface. The third metal surface is an electrochemically microstructured aluminum surface used for building condensers (Table 3). The metal foils were hydrophobized with Dynasylan (according to Table 2).

Scanning Electron Microscopy. All specimens were fixed to aluminum stubs, sputter-coated (Balzer Union SCD 040, Balzer-Pfeifer GmbH, Asslar, Germany), and examined in a LEO 440 i (LEO Electron Microscopy, Ltd., Cambridge, U.K.).

Contact Angle Measurements. The equilibrium water contact angle on the prepared surfaces was measured by a contact angle meter (Goniometer G1, Krüss GmbH, Hamburg, Germany). The volume of the applied droplets of distilled water was $15 \mu\text{L}$. The mean value was calculated from at least eight individual measurements.

Sliding Angle Measurements. To measure the sliding angle, at first a water drop (distilled water, $V = 15 \mu\text{L}$) was applied on the specimen fixed to a tiltable plate. Then the plate was inclined slowly, until the drop started to move. The sliding angle was determined on a scale with a precision of 0.5° . Depending on the variation of the data, the mean value was calculated from 5 to 12 individual measurements.

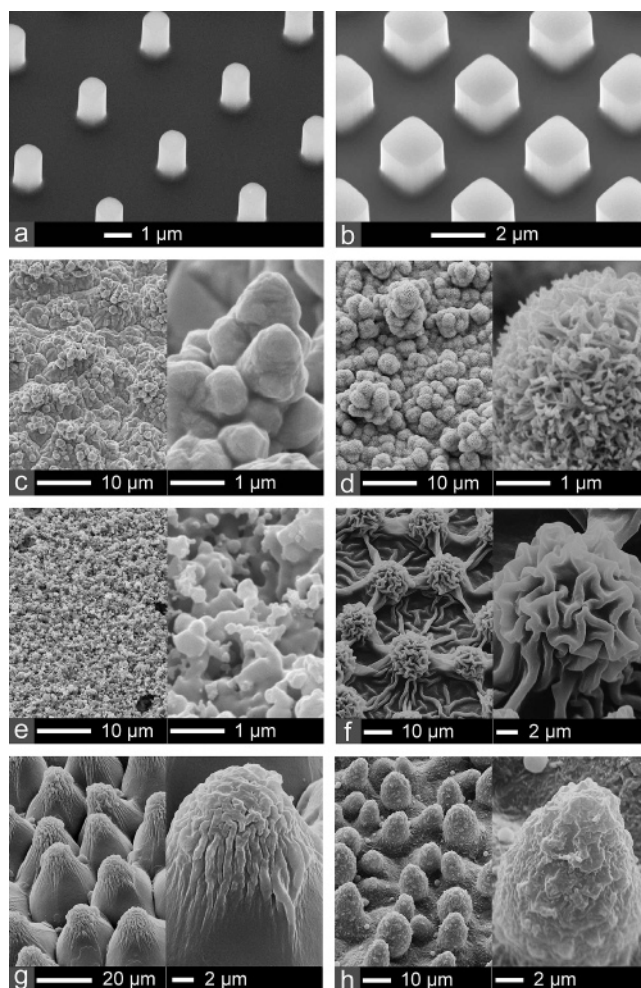


Figure 1. (a–h) SEM photographs of microstructured water-repellent surfaces: (a, b) silicon chips with regular patterns of spikes, (c) copper foil Cu-1, (d) copper foil Cu-2, (e) aluminum foil Al-1, (f) replicate of *Alocasia*, (g) replicate of *Rosa*, and (h) replicate of *Nelumbo*.

Table 2. Designations and Descriptions of the Different Methods Used for Hydrophobizing Silicon Wafers and Metal Surfaces

designation	description of hydrophobizing
Au-thiol	gold sputtering for 40 s and hydrophobizing with a solution of 1 vol % 1-hexadecanethiol (Merck-Schuchard, Hohenbrunn, Germany) in heptane (Carl Roth, Karlsruhe, Germany); time of immersion, 30 min
Dynasylan	solution of 4.8 vol % Dynasylan F 8815 (fluoroalkylfunctional waterborne oligosiloxane; Degussa, Frankfurt/Main, Germany) in methanol (Carl Roth, Karlsruhe, Germany); time of immersion, 5 min; following heat treatment at 100°C for 1 h

Artificial Contamination and Artificial Rinsing. A luminescent and hydrophobic powder was used as a contaminant. This powder was made by mixing half-and-half luminescent material (Leuchtstoff Farbe 20, Osram, Schwabmünchen, Germany) and a fluorinated agent (Antispreed F 2/50 FK 60, Dr. Tilwich, Horb, Germany) and evaporating the solvent.

The specimens had a size of approximately 20×30 mm, except for the silicon samples. They were fixed to aluminum stubs with double-sided adhesive tape and placed in a chamber measuring $28 \times 28 \times 75$ cm. The chamber was divided by a removable horizontal wooden plate 15 cm above the ground covering the specimens. A total of 0.5 g of the contaminant was filled in a bowl placed near the top of the chamber. The powder was dispersed by a fan. After 5 s the fan was turned off, and the wooden plate

Table 3. Designations for the Replicates of Plant Surfaces and for the Metal Surfaces Used for the Experiments

designation	description of the surface
<i>Alocasia</i>	replicate of leaf of <i>A. macrorrhiza</i> (abaxial leaf side)
<i>Rosa</i>	replicate of petal of <i>R. landora</i>
<i>Nelumbo</i>	replicate of leaf of <i>N. nucifera</i> (lotus plant)
<i>Cu-1</i>	microstructured copper foil (CF 35 μ NT-TO, Circuit Foil Luxembourg, Wiltz, Luxembourg)
<i>Cu-2</i>	microstructured copper foil with CuO crystals [Bolta 18 μ m BO, R_a = 2.4–2.8 μ m (Bolta-Werke, Gottmadingen, Germany)]
<i>Al-1</i>	microstructured aluminum foil (Becromal LD 888 F 86V, Frolyt, Freiberg, Germany)

was removed. Subsequently the particles evenly deposited on the specimens.

Following contamination, the specimens were subjected to artificial fog and rain. Fog treatment was performed in a chamber equipped with a high-pressure fog system (HNS, Osberma, Engelskirchen, Germany) producing very fine droplets in the diameter range of 8–20 μ m. Inside the chamber the specimens were attached to a tilted stage (tilting angle, 45°). The treatment lasted 5 min (water quantity, 1500 mL/m²); after an additional 55 min, the specimens were put into a drying oven to remove some small drops remaining on the specimens.

Water droplets larger than 2 mm could be produced by means of a sprinkler. The sprinkler head consisted of a vessel with an array of 24 needles (internal diameter D = 0.9 mm; area, 2 \times 2 cm) at the bottom. From the top, water was supplied continuously into the vessel to keep a constant water level. The specimens were moved slowly back and forth underneath the sprinkler to cover the complete surface with droplets. The distance between the needles and the specimen was varied. As the specimen was tilted slightly remaining water could run off quickly.

Afterward the specimens were sputter-coated and examined in a SEM (Cambridge Stereoscan 200, Cambridge Instruments, Cambridge, U.K.) equipped with a cathodoluminescence detector able to distinguish the contaminants from the surface structures. For each SEM image (size, approximately 280 \times 180 μ m) the total area (i.e., projected area) of the contaminating particles was determined using imaging processing software. All contamination values of a specimen (eight altogether) were added up so that the total examined area was approximately 0.40 mm². The mean value was calculated from the values of four specimens and then divided by a standardized starting contamination (calculated from 10 specimens), thus, getting the remainder of the contamination.

For almost perfectly cleaned surfaces the remainder of contamination is not very suitable to characterize the cleanliness because it largely depends on the size of very few particles. Therefore, a degree of cleanliness was defined. For each surface it is the number of SEM images without any contaminating particle within these images divided by the total number of images. By examining three or four specimens, 30–40 images were made per surface. A surface area of 0.05 mm² was covered with each image.

Results and Discussion

Silicon Wafer Specimens with Regular Patterns of Spikes. On superhydrophobic substrates a water drop generally forms a sphere. Water does not intrude into the valleys between the microstructures, and air is entrapped between the drop and the solid forming what has been called a “composite surface”. With the formula of Cassie and Baxter² the apparent contact angle θ_m can be calculated from the equilibrium contact angle of the flat surface θ (of the same nature) and the solid fraction Φ_s , that is, the area fraction of the liquid–solid contact:

$$\cos \theta_m = -1 + \Phi_s(\cos \theta + 1) \quad (1)$$

On such surfaces the hysteresis, that is, the difference

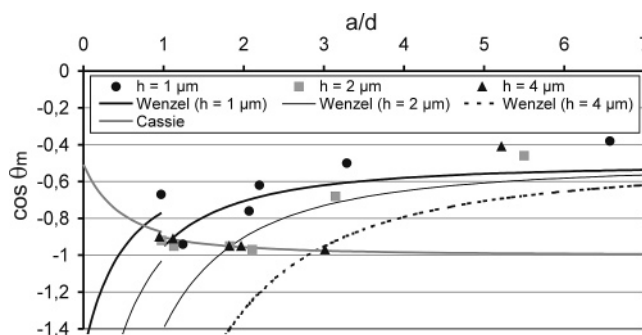


Figure 2. Water contact angles θ_m of hydrophobized silicon chips with regular patterns of spikes (whose width d , clearance a , and height h were varied) as a function of a/d , compared with the plots of θ_m for Wenzel and Cassie drops. For $a/d < 1$ the calculations were made for spikes with a 2- μ m-wide square base, and for $a/d > 1$ the spikes represented 0.9- μ m-wide cylinders.

between the advancing contact angle θ_a and the receding contact angle θ_r is low. As a result also the sliding angles are small. This relationship between hysteresis and the sliding angle is described by the formula of Furmidge²¹

$$\sin \alpha_r = \frac{\sigma_{lv} w}{mg} (\cos \theta_r - \cos \theta_a) \quad (2)$$

where α_r is the sliding angle, m is the weight of the water droplet, w is the width of the droplet, and σ_{lv} is the interfacial tension of the water at the water–air interface.

A drop on a rough hydrophobic substrate can occupy a second equilibrium state which can be called the Wenzel state. In this case the drop wets the whole microstructure. The apparent contact angle θ_m is then a function of the surface roughness r (the ratio of the actual to the apparent surface area of the substrate) and the contact angle θ :³

$$\cos \theta_m = r \cos \theta \quad (3)$$

We varied the solid fraction of a model system, silicon samples with regular patterns of spikes (see also Figure 1a,b), by using six geometrical designs with different widths of the spikes and distances between them. Furthermore, for all these geometries the height of the structures was varied.

Figure 2 shows the equilibrium water contact angle on these substrates as well as the plots of the formulas of Cassie and Wenzel as a function of the geometric parameter a/d (where d is the width of the spikes and a is the clearance between them). The calculation of the theoretical curves were made for two types of spikes. For $a/d < 1$ we assumed 2- μ m-wide prisms with a squared top side because the silicon chips of design d_2a_2 (Figure 1b) have a a/d value slightly below 1. The spikes of the silicon chips with designations d_1a_1 to d_1a_5 (Figure 1a, d_1a_3) have nearly a circular top side, so we used 0.9- μ m-wide cylinders as the model system for $a/d > 1$.

It can be seen that the measured contact angles of the specimens with 4- μ m-high spikes are in good agreement with the theoretical curve for Cassie drops, except for the value for design d_1a_5 . When $a/d < 3$ the apparent contact angle θ_m for the Cassie state is lower than for the Wenzel state; the composite state represents a global minimum in energy. However, the measured values of θ_m on all surfaces with only 1- μ m-high structures and on some of the surfaces with 2- μ m-high structures are quite close to the theoretical curve for Wenzel drops. In having a lower

(21) Furmidge, C. G. L. *J. Colloid Sci.* **1962**, *17*, 309.

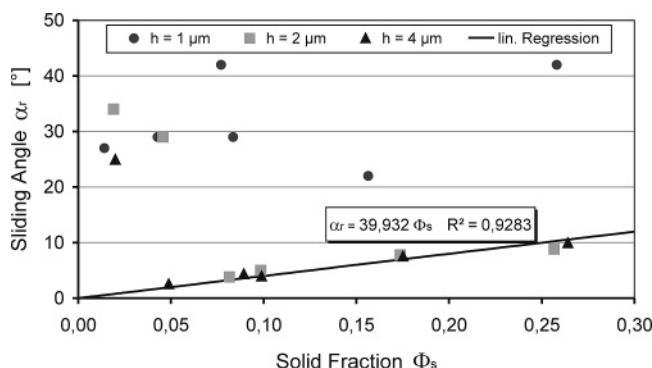


Figure 3. Sliding angle of water drops on hydrophobized silicon chips with regular patterns of spikes (whose width, clearance, and height were varied) as function of the solid fraction Φ_s .

contact angle as Cassie drops, their formation is energetically favorable. This is due to the moderate roughness r of these substrates. The Cassie regime is stabilized if

$$\cos \theta + 1/r < 0 \quad (4)$$

which is a simplified criterion for designing superhydrophobic self-cleaning surfaces.⁸ Our results are in accordance with the modeling of contact angles on rough hydrophobic surfaces performed by Patankar.¹⁰ In his latest report¹¹ he suggested also slender pillars as a suitable microroughness for self-cleaning superhydrophobic surfaces on which the formation of Cassie drops is energetically preferred. Even though the 4- μm -high spikes in our experiments are not very slender, the results are in a way a verification for Patankar's prediction.

Some contact angle values are near the intersection of the Wenzel and the Cassie curves. To decide whether a drop formed a wetted or a composite contact to the specimen we considered the results of the sliding angle measurements (Figure 3). Drops on surfaces with 4- μm -high spikes usually rolled off at angles less than 10°. There is a linear correlation between the sliding angle and the solid fraction. The lower this fraction, the lower the sliding angle. But again, the behavior of water droplets on many of the specimens with 1- and 2- μm spikes was different; they did not start to move until the angle of inclination was above

Table 5. Degree of Cleanness of Hydrophobized Silicon Chips with Regular Patterns of Cylindrical Spikes (Height, 4 μm) after Artificial Contamination and Rinsing

designation	degree of cleanness [%]	designation	degree of cleanness [%]
d_1a_1	90	d_1a_3	95
$d_1a_{1.5}$	90	d_2a_2	87.5
d_1a_2	100		

20°, up to over 40°. That is, on those substrates water drops exhibit a high hysteresis (according to formula 2) which is an indication for being in the Wenzel state.⁸ We assumed the Cassie state if the sliding angle was not higher than 10°. This was compared with the criterion above (Table 4). As expected, a complete wetting according to Wenzel occurred only if the left-hand side of formula 4 was positive. If the criterion is fulfilled, a high water repellency in accordance with Cassie's model was always found. However, this phenomenon could be observed also in some cases when the value of formula 4 was slightly above 0 because metastable Cassie states are possible in the Wenzel region.⁸

Five different surfaces, all designed with 4- μm -high spikes and hydrophobized, were subjected to a self-cleaning test. These specimens could be cleaned almost completely by the artificial fog. The degree of cleanness (for a definition, see Experimental Section) was at least 87.5%; that is, on the vast majority of SEM images no contamination particles could be detected (Table 5). During the fog treatment the fog droplets form macroscopic water drops that roll off the inclined specimen removing the contamination particles lying on the tips of the microstructure. Because the smallest particles were larger than 1 μm only very few particles fell into the valleys between the spikes, where a removal by water drops without kinetic energy, in contrast to rain drops, is nearly impossible.

Replicates of Plant Surfaces. Tests with replicates of plant surfaces instead of original leaves allow separate studies of the influence of geometry and surface chemistry on water repellency. The leaves of *Alocasia macrorrhiza* and the petals of *Rosa landora*, both showing cuticular folds, could almost perfectly be replicated (Figure 1f,g; the replicates are in the following described as "Alocasia"

Table 4. Solid Fraction Φ_s , Surface Roughness r , Contact Angle (CA) θ_m , and Sliding Angle (SA) α_r of Hydrophobized Silicon Chips with Regular Patterns of Spikes, Compared with the Theoretical Values $\theta_{m,w}$ and $\theta_{m,c}$ According to the Formulas of Wenzel and Cassie, Respectively^a

geometric dimensions				theoretical CAs		experimental results			critereon
h	design	Φ_s	r	$\theta_{m,w}$ [deg]	$\theta_{m,c}$ [deg]	CA θ_m [deg]	SA α_r [deg]	model	$\cos \theta + 1/r$
1	d_1a_1	0.156	1.7	152	157	161	22	Wenzel	0.07
1	$d_1a_{1.5}$	0.084	1.4	137	164	139	29	Wenzel	0.19
1	d_1a_2	0.077	1.3	133	164	128	42	Wenzel	0.24
1	d_1a_3	0.043	1.2	128	168	120	29	Wenzel	0.33
1	d_1a_5	0.014	1.1	123	173	113	27	Wenzel	0.42
1	d_2a_2	0.258	1.5	141	164	132	42	Wenzel	0.14
2	d_1a_1	0.174	2.6	156	156	161	8	Cassie	-0.12
2	$d_1a_{1.5}$	0.098	1.9	169	162	162	5	Cassie	0.01
2	d_1a_2	0.081	1.7	151	164	165	4	Cassie	0.08
2	d_1a_3	0.046	1.4	135	168	133	29	Wenzel	0.21
2	d_1a_5	0.019	1.2	127	172	118	34	Wenzel	0.35
2	d_2a_2	0.257	2.1	151	151	157	9	Cassie	-0.02
4	d_1a_1	0.175	4.1	156	156	156	8	Cassie	-0.27
4	$d_1a_{1.5}$	0.099	2.9	162	162	162	4	Cassie	-0.16
4	d_1a_2	0.089	2.5	163	163	161	4	Cassie	-0.11
4	d_1a_3	0.049	1.8	157	167	166	3	Cassie	0.04
4	d_1a_5	0.020	1.4	134	172	114	25	Wenzel	0.23
4	d_2a_2	0.264	3.1	151	151	154	10	Cassie	-0.19

^a The width d , the clearance a , and the height h of the spikes were varied. On the basis of the measured sliding angles, it was decided whether the water drops were in the Cassie or the Wenzel state. This was compared with theory, which says that the Cassie regime is fulfilled if $\cos \theta + 1/r < 0$.

Table 6. Contact Angle θ_m and Sliding Angle (Mean Value \pm Standard Deviation) of Replicates of Plant Surfaces Made of a Hydrophobic Polymer

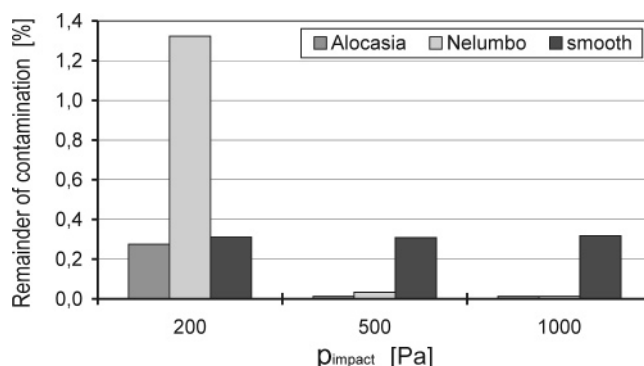
designation	contact angle [deg]	sliding angle [deg]
<i>Alocasia</i>	154.4 \pm 2.0	11.2 \pm 1.9
<i>Rosa</i>	151.7 \pm 4.3	7.3 \pm 1.6
<i>Nelumbo</i>	157.8 \pm 4.2	7.9 \pm 2.8

and “*Rosa*”). In contrast, the wax crystals of the lotus leaf (*Nelumbo nucifera*) could not be replicated because they were too delicate (about 200 nm in diameter). However, the replicated papillae (convex epidermal cells) exhibit a scalelike roughness in the range of 1–3 μ m (Figure 1h; the replicate is in the following described as “*Nelumbo*”).

Despite the missing structure of the wax crystals, the water contact angle of *Nelumbo* is the highest of all the replicates (Table 6) indicating that the microstructure formed by the papillae alone is already optimized with regard to water repellency. The papillae of *Alocasia* are spherical consisting of approximately 1- μ m-wide cuticular folds. These folds are more pronounced than those on the papillae of *Rosa*. As a result, water drops on *Alocasia* exhibit a higher contact angle than on *Rosa*. Nevertheless the sliding angle on *Alocasia* is the highest, which remains to be explained.

Rinsing of *Nelumbo* with artificial fog resulted in a continuous water film on the surface. This can be explained by the almost absent structure in the range below 5 μ m. Then tiny fog droplets (diameter range, 8–20 μ m) falling into the valleys between the papillae are not repelled and gradually replace the air enclosed within the microstructure. As a result, the surfaces are not self-cleaning. After contamination and fog treatment the particles were evenly spread on the specimens forming a veil visible to the naked eye. In contrast to that, natural leaves of lotus behave differently when being subjected to artificial fog. Fog droplets fuse to form bigger drops, which are elevated by the structure and finally roll off the specimens taking along contaminating particles. This demonstrates clearly that the fine structure on the papillae of natural lotus represented by wax crystals leads to a different wetting behavior compared to a surface only having the coarse structure represented by the papillae; both materials, natural wax and polymer used for the replicates, have a similar hydrophobicity. These results are in good accordance with the calculations of Patankar¹¹ who showed that double roughness structures are appropriate surface geometries to develop self-cleaning surfaces on which Cassie drops are always formed. Similar to natural lotus the replicates of *Alocasia* and *Rosa* were cleaned by artificial fog. Obviously the cuticular folds prevent *Alocasia* and *Rosa* from being wetted completely. The remainder of contamination was 0.4% on *Alocasia* and 3.1% on *Rosa*, respectively. We attribute the less effective self-cleaning of *Rosa* to its less-pronounced structure; the lower parts of the papillae are even smooth.

In contrast, all specimens were cleaned when subjected to artificial rain. The amount of contaminating particles remaining after rain treatment depends on the kinetic energy of the drops hitting the specimens' surface. The higher the drops' kinetic energy and, thus, their impact pressure on the surface, the more perfectly the specimens were cleaned (Figure 4). When the impact pressure was 1000 Pa, that is, the dynamic pressure of droplets impinging on the surface from a given height, all contamination was removed totally. It was questioned whether an artificial rain shower would also be able to clean a smooth hydrophobic surface the same way. Therefore, the same experiments were performed with

**Figure 4.** Remainder of contamination on replicates of two plant surfaces and one smooth surface made of a hydrophobic polymer after sprinkling with water drops. The kinetic energy and, therefore, the impact pressure of the drops were varied.**Table 7. Contact Angle (Mean Value \pm Standard Deviation) θ of Perfectly Smooth Silicon Chips Hydrophobized with Different Agents and of a Smooth Surface of the Polymer Used for the Replicates**

designation	contact angle [deg]
Au-thiol	120.6 \pm 3.2
Dynasylan	111.9 \pm 2.4
polymer used for the replicates	102.9 \pm 4.5

Table 8. Contact Angle θ_m and Sliding Angle (Mean Value \pm Standard Deviation) of Metal Foils Hydrophobized with Dynasylan

designation	contact angle [deg]	sliding angle [deg]
<i>Cu</i> -1	158.2 \pm 3.2	7.3 \pm 1.5
<i>Cu</i> -2	164.8 \pm 2.5	0.5
<i>Al</i> -1	151.8 \pm 2.9	7.4 \pm 1.6

smooth specimens made of the same polymer as the replicates (for contact angle, see Table 7). When the impact pressure was only 200 Pa, the remainder of contamination on the smooth specimens was similar to that of *Alocasia*, but this value remained almost constant even for higher impact pressures. This demonstrates the distinct difference between the self-cleaning property of many superhydrophobic surfaces and the limited ability of smooth hydrophobic surfaces, often called “easy to clean”, to be decontaminated by drop impact only.

Microstructured Metal Foils. For our investigations three different metal foils were used, hydrophobized with Dynasylan.

Cu-2 has a combination of microstructures on different length scales. Spherical structures measuring approximately 3 μ m are covered by fine crystals of copper oxide. This combined structure leads to a considerable reduction of the contact area between the surface and the water droplets. The contact angle was 165° (Table 8), the highest value of all surfaces presented in this paper. On this surface, it was not possible to measure the sliding angle. All drops rolled off the surface after their application onto the horizontal specimen. The indicated value of 0.5° lies within the range of the measuring error.

A combined structure can also be found on *Cu*-1: approximately 10- μ m-wide pyramids are covered with spherical structures measuring 1–2 μ m. This microstructure is not as porous as that of *Cu*-2; the solid fraction is higher and less air is enclosed between the structures. As a result the water contact angle is only about 158° and the sliding angle lies above 7°.

The contact angle of *Al*-1 is the lowest of all metal surfaces presented here. *Al*-1 has no combined structure; the microstructure consists of irregularly formed struc-

Table 9. Remainder of Contamination (Mean Value \pm Standard Deviation) of Metal Foils Hydrophobized with Dynasylan after Artificial Contamination and Rinsing

designation	remainder of contamination [%]
<i>Cu</i> -1	0.58 ± 0.24
<i>Cu</i> -2	1.74 ± 1.17
<i>Al</i> -1	0.02 ± 0.04

tures in the range of $0.2\text{--}1\text{ }\mu\text{m}$. The sliding angle is comparable with that of *Cu*-1. Obviously the lack of coarse structural elements besides the structures on the sub-micrometer scales has a negative effect on water repellency.

After contamination and exposure to artificial fog, more than 98% of the contaminations on the metal surfaces could be removed. All metal foils have a pronounced roughness and exhibit surface structures smaller than $2\text{ }\mu\text{m}$, in particular in the valleys between the coarser structures. As a result, also fine fog droplets are repelled (in contrast to the replicates of *Nelumbo*). Such small droplets merge to macroscopic drops which are elevated by the structure and then roll off. We found almost no remainder on the specimen of *Al*-1 (Table 9), most obviously because of the lack of coarse structural elements. In contrast to that, the surfaces of *Cu*-1 and *Cu*-2 could not be cleaned completely by artificial fog. Water drops formed by the coalescence of tiny fog droplets had no kinetic energy to get into all the valleys between the coarse structures where some of the contaminating particles were deposited. If sprinkled with artificial rain, also these surfaces can be cleaned perfectly. These results correspond to earlier investigations on the self-cleaning properties of superhydrophobic plant surfaces where the leaves of *Brassica oleracea* (cabbage) were cleaned by fog very well, too.¹ The leaves of *Brassica* also only have structures (wax crystals) measuring about $1\text{--}5\text{ }\mu\text{m}$.

Summary

The wetting and the self-cleaning properties of three types of superhydrophobic surfaces have been investi-

gated: silicon wafer specimens with different periodic arrays of spikes which were made hydrophobic by chemical treatment, replicates of water-repellent leaves of plants, and finally industrially fabricated metal foils additionally hydrophobized by means of a fluorinated agent. Drops of water rolled off easily from silicon samples with a microstructure consisting of rather slender and sufficiently high spikes with an appropriate pitch; this is attributed to the fact that the space between the spikes remains filled with air. These samples could be cleaned after artificial contamination by means of fog treatment almost completely. On surfaces with low spikes and a rather high pitch the behavior of water drops was different; that is, we found a considerable decrease of the contact angles and a distinct rise in the sliding angles; in these cases obviously the specimen has a larger contact area to the drop surface.

Some metal foils and some replicates had two levels of roughness; as a result, a total removal of all contaminating particles was not possible when subjected to artificial fog, but water drops impinging with sufficient kinetic energy could clean these surfaces perfectly. A substrate where pronounced structures in the range below $5\text{ }\mu\text{m}$ were lacking could not be cleaned by means of fog consisting of water droplets (diameter range, $8\text{--}20\text{ }\mu\text{m}$) because this treatment resulted in a continuous water film on the samples. However, artificial rain removed all the contamination. On the other hand smooth specimens made of the same material could not be cleaned completely by impinging droplets. This is a clear indication of the different contact phenomena on smooth hydrophobic in contrast to self-cleaning microstructured surfaces, for which the term "Lotus-Effect" often is used.

Acknowledgment. The authors gratefully acknowledge funding of the project by the Deutsche Bundesstiftung Umwelt.

LA0401011